Virology 444 (2013) 203–210

Contents lists available at ScienceDirect

Virology

journal homepage: www.elsevier.com/locate/yviro

Characterization of a nuclear localization signal in the foot-and-mouth disease virus polymerase

Maria Teresa Sanchez-Aparicio [a,1], Maria Flora Rosas [a], Francisco Sobrino [a,b,*]

[a] Centro de Biología Molecular, "Severo Ochoa" (CSIC-UAM), Cantoblanco 28049, Madrid, Spain
[b] Centro de Investigación en Sanidad Animal, INIA, Valdeolmos, 28130 Madrid, Spain

ARTICLE INFO

Article history:
Received 30 April 2012
Returned to author for revisions
25 May 2012
Accepted 10 June 2013
Available online 22 July 2013

Keywords:
NLS
FMDV
Viral polymerase

ABSTRACT

We have experimentally tested whether the MRKTKLAPT sequence in FMDV 3D protein (residues 16 to 24) can act as a nuclear localization signal (NLS). Mutants with substitutions in two basic residues within this sequence, K18E and K20E, were generated. A decreased nuclear localization was observed in transiently expressed 3D and its precursor 3CD, suggesting a role of K18 and K20 in nuclear targeting. Fusion of MRKTKLAPT to the green fluorescence protein (GFP) increased the nuclear localization of GFP, which was not observed when GFP was fused to the 3D mutated sequences. These results indicate that the sequence MRKTKLAPT can be functionally considered as a NLS. When introduced in a FMDV full length RNA replacements K18E and K20E led to production of revertant viruses that replaced the acidic residues introduced (E) by *K*, suggesting that the presence of lysins at positions 18 and 20 of 3D is essential for virus multiplication.

Introduction

Foot-and-mouth disease virus is a member of the *Picornaviridae* family and the causative agent of an acute vesicular disease affecting pigs, ruminants and other cloven-hoofed livestock (Kitching, 2005; Sáiz et al., 2002). Viral genome consists of a single-stranded positive-sense RNA molecule of about 8.5 kb in length with the 5′end covalently linked to the viral protein VPg, and a poly A tract at the 3′ end. The viral products are translated from a single open reading frame which is flanked by two non-coding regions (NCRs) containing specific structures involved in the control of replication and translation of the viral genome. Translation of the ORF begins with the proteinase Lpro, which is followed by the capsid proteins (1A, 1B, 1C, and 1D), a short autoproteinase (2A), and the remaining nonstructural proteins (2B, 2C, 3A, 3B, 3C, and 3D). 3C is responsible for most of the cleavage sites in the FMDV polyprotein (Ryan et al., 2004), leading to the mature viral proteins as well as different precursors found in infected cells, and 3D is the core subunit of the RNA-dependent RNA polymerase (Newman et al., 1979).

Despite picornavirus multiplication occurring in the cytoplasm of infected cells, recent evidences indicate that these viruses can alter the nucleus cytoplasm traffic, and reprogram the nucleus of host cells (Belov et al., 2000; de los Santos et al., 2009; Groppo et al., 2011; Gustin and Sarnow, 2001). Picornavirus infections can alter the subcellular localization of certain nuclear RNA-binding proteins. For example, enteroviruses trigger the re-localization of poly-C binding protein (PCBP2), nucleolin, and polypyrimidine tract binding protein (PTB) from the nucleus to the cytoplasm. Once in the cytoplasm, some of these proteins interact with viral RNA and proteins, thus contributing to the virus replication cycle.

Several evidences support the interactions between FMDV proteins and the cell nucleus and the alterations they cause. During FMDV infection of cultured cells, 3C mediates cleavage of histone H3 (Falk et al., 1990; Grigera and Tisminetzky, 1984). On the other hand, RNA helicase A (RHA) (Lawrence and Rieder, 2009) and Sam68, both RNA-binding proteins relevant for viral life cycle, are redistributed from the nucleus to the cytoplasm of infected cells (Lawrence et al., 2012). Also, Lpro is translocated to the nucleus where it mediates degradation of p65/RelA, a subunit of NF-κB (de Los Santos et al., 2007), which is associated with the inhibition of the induction of IFN-β mRNA and the expression of IFN-α/β-stimulated genes in swine cells (de Los Santos et al., 2006). A recent report has described the suppression of dsRNA-induced IFN-β transcription through degradation of interferon regulatory factor 3/7 by Lpro (Wang et al., 2010). On the other hand, FMDV 3D and its precursor 3CD localize in the nucleus of infected cells and in cells transiently expressing each of these proteins (García-Briones et al., 2006). Delivery of 3C in the cell nucleus as part of the 3CD precursor would facilitate the 3C-mediated histone H3

* Corresponding author. Fax: +34 91 1964420.
E-mail address: fsobrino@cbm.uam.es (F. Sobrino).
[1] Department of Microbiology, Icahn School of Medicine at Mount Sinai, New York, NY 10029, USA

0042-6822/$ - see front matter © 2013 Elsevier Inc. All rights reserved.
http://dx.doi.org/10.1016/j.virol.2013.06.011

cleavage occurring upon infection (Falk et al., 1990). Here, we report that the sequence at the N-terminus of 3D (residues 16 to 24), predicted as potential nuclear localization signal (NLS) by its homology with related signals reported for other picornavirus (Aminev et al., 2003b; Amineva et al., 2004), actually acts as a NLS.

Results and discussion

Mutations in basic residues of the MRKTKLAPT motif decrease the nuclear localization of FMDV 3D protein

The primary sequence of the N-terminus of FMDV 3D of the 7 different FMDV serotypes shows an amino acid motif MRKTKLAPT corresponding to residues 16 to 24 (Carrillo et al., 2005). This motif is conserved among other picornaviruses, such as EMCV and rhinovirus (Aminev et al., 2003a; Amineva et al., 2004) and fits the consensus sequence for NLS from yeast ribosomal proteins (YRP-NLS) (Stuger et al., 2000) (Fig. 1). Basic residues are defined as important for NLS recognition by importin proteins (Nigg, 1997; Stuger et al., 2000; Terry et al., 2007). To explore whether the MRKTKLAPT motif was involved in 3D nuclear localization and approach similar to that used by Aminev et al. (2003a, b) was followed. Thus, point mutations in two of the three basic residues herein (K18E and K20E) were introduced in pRSV derivatives. The expression levels of 3D in BHK-21 cells transfected with plasmids pRSV3DK18E, pRSVDK20E and pRSV3Dwt were found similar by western blotting (data not shown). To study the cellular distribution of the mutant proteins, transfected cells were fixed and stained with a 3D-specific antiserum. As reported (García-Briones et al., 2006), 3Dwt was visualized with a similar intensity at both the cytoplasm and the nucleus of transfected cells by confocal microscopy (Fig. 2A). Conversely, in cells expressing the mutant proteins 3DK18E and 3DK20E, fluorescence was mainly observed in the cytoplasm, being their nuclear staining lower than that of 3Dwt. When the subcellular expression of 3D protein was quantified, the proportion of cells showing a staining intensity similar between cytoplasm and nucleus was significantly higher ($p < 0.05$) in cells expressing 3Dwt (95% of stained cells) that in those expressing the 3D mutants (Fig. 2B). These differences were higher for K20E than for K18E mutant protein. About 60% of the cells expressing 3DK18E showed a similar intensity staining between cytoplasm and nucleus and around 40% of the cells showed a cytoplasmic fluorescence higher than that observed in the nucleus, while for the mutant 3DK20E about 10% of the cells showed a similar intensity staining between cytoplasm and nucleus and around 90% of the cells showed a cytoplasmic fluorescence higher than that observed in the nucleus (Fig. 2B). We next analyzed the presence of 3D protein in the cytoplasmic and the nuclear fractions, obtained by differential centrifugation, by western blot from cells transfected with the different pRSV3D plasmids. As shown in Fig. 2C, the amount of 3Dwt protein detected was similar in both fractions, while 3D mutants were mainly observed in the cytoplasmic fraction. The specificity of this cell fractionation was supported by the low amount of βII-tubulin detected in the nuclear fraction, while signal to the nuclear envelope protein lamine A/C was mainly present in this fraction. These results indicate that replacements K18E and K20E can alter cellular distribution of FMDV 3D protein transiently expressed in BHK-21 cells. Similar results were observed in Vero cells transfected with the same plasmids (data not shown). The role of the third basic residue (R17) present in the MRKTKLAPT motif on the nuclear location of 3D remains to be studied.

Mutations K18E and K20E decrease the nuclear localization of FMDV precursor 3CD

The nuclear localization of the 3CD precursor has been described in cells infected with picornaviruses (Amineva et al., 2004; Weidman et al., 2003), including FMDV (García-Briones et al., 2006). To explore whether this nuclear localization could be affected by mutations K18E and K20E, three additional pRSV derivatives were constructed: pRSV3CDwt, pRSV3CDK18E and pRSV3CDK20E. No expression was observed by immunofluorescence in cells lypofectamine-transfected with plasmids 3CDwt or their mutant versions (data not shown), which could be due to the cell toxicity induced by 3C (Martínez-Salas and Domingo, 1995). Upon transfection of cells by electroporation, 3CD proteins were detected by westernbloting (Fig. 3A) As observed for 3D mutants, fluorescence to 3CDK18E and 3CDK20E mainly localized in the cytoplasm of transfected cells, whereas that of 3CDwt appeared evenly distributed in the cytoplasm and the nucleus (see Fig. 3B). Subcellular fractions of BHK-21 transfected cells showed a distribution of the 3CD proteins similar to that observed by immunofluorescence (Fig. 3C). In this case, 3CDwt was detected in both nuclear and cytoplasmic fractions, in which 3Dwt was also observed, as a result of the precursor processing. On the other hand, 3CDK18E and 3CDK20E mutant proteins were only detected at the cytoplasmic fraction, probably reflecting an impairment in their nuclear import, as that observed for 3D mutant proteins.

Peptide MRKTKLAPT can target a heterologous protein to the nucleus of transfected cells and mutations K18E and K20E decrease this targeting

To confirm that MRKTKLAPT motif could directly mediate nuclear protein transport, its corresponding sequence was cloned as a C-terminal fusion with the green fluorescent protein (GFP). Plasmids expressing fusion proteins GFPNLSwt, GFPNLSK18E, GFPNLSK20E, as well as GFPNLSsv40 – that harboured a fusion of GFP with the NLS of SV40 large T antigen (Conti et al., 1998; Kalderon et al., 1984), which was included as control of nuclear targeting – were constructed (Fig. 4A). Plasmid pGFP expressing the marker protein alone was included as control. Upon 24 h post

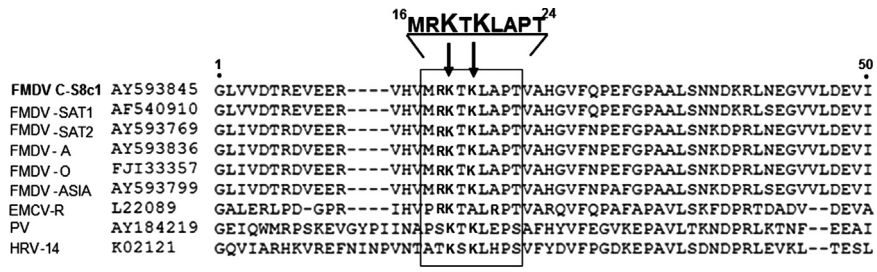

Fig. 1. Localization of the putative NLS in the different FMDV serotypes. Alignment of the amino acid sequences corresponding to the 3D amino terminus from FMDV, PV, HRV and EMCV. The sequence MRKTKLAPT, corresponding to the consensus NLS found in several yeast ribosomal proteins – [*G*/*P*] (*K*/*R*)$_3$ X1–4 [*G*/*P*] – (Aminev et al., 2003b; Stuger et al., 2000), is indicated and the alignment of these residues resalted in box in which basic residues are highlighted.

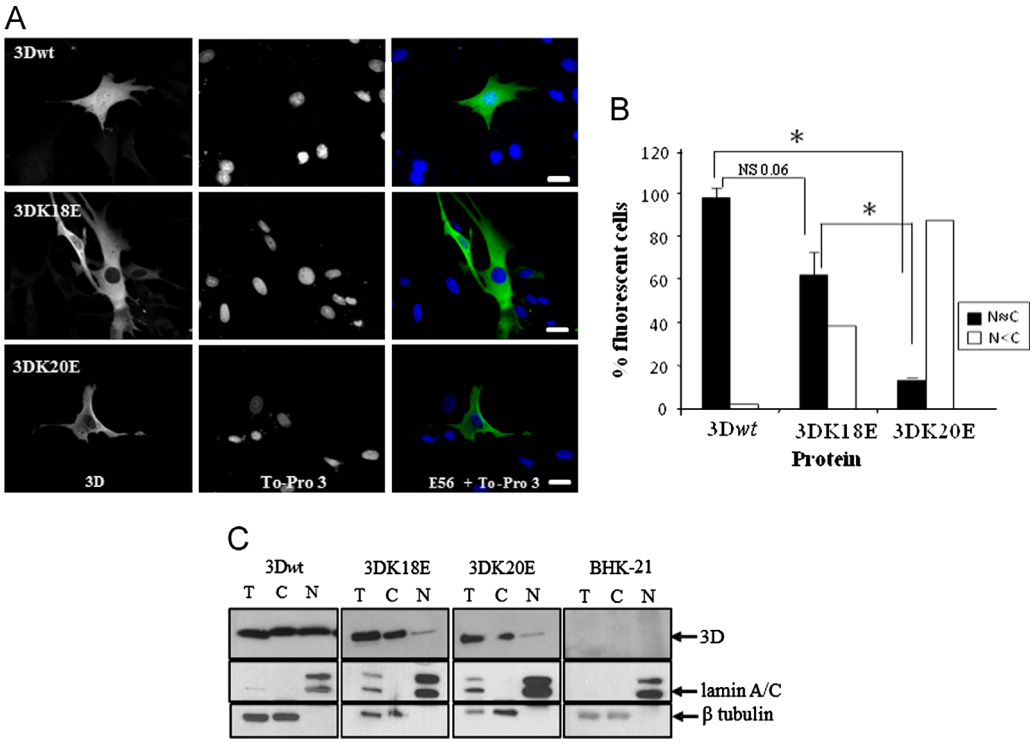

Fig. 2. Expression and cellular localization of 3Dpol harboring mutations K18E and K20E. BHK-21 cells were transfected with pRSV-3D, pRSV-3DK18E or pRSV-3DK20E and collected at 24 h post transfection. (A) Confocal images of 3D distribution. Expression of 3D was detected with serum E56 and Alexa Fluor 488 anti-rabbit IgGs as secondary antibody; nuclei were stained with To-Pro3. Scale bar: 20 μm. (B) Quantitative estimation of the localization of the 3D wt or mutants 3DK18E and 3DK20E. A number of 150 fluorescence-positive cells were scored as: $N \approx C$ (when similar nuclear and cytoplasmic staining was observed) or $N < C$ (when the percentage of nuclear immunofluorescence was less than 50% of that observed in the cytoplasm). Asteriscs (*) indicate significant differences ($p < 0.05$). (C) Western blot analysis of cellular fractions of BHK-21 cells transfected with 3D pRSV derivatives. At 20 h post infection, total cell extracts (*T*), cytoplasmic and cell membrane fraction (*C*) and nuclear fraction (*N*) were obtained and blotted (as described in Materials and methods). The migration of the markers and their molecular weight are indicated. Arrows point to the bands corresponding to 3D, βII-tubulin and lamin A/C.

transfection with the different plasmids, the localization of GFP fluorescence in BHK-21 cells was monitored by confocal laser scanning microscopy. As reported (Garrido-Garcia et al., 2009), expression of GFP alone was detected homogeneously throughout the transfected cells, with a pattern similar to that observed for mutants GFPNLSK18E and GFPNLSK20E (Fig. 4B). On the contrary, expression of GFP-NLS showed an increased nuclear distribution similar to the found for GFPNLSsv40 expression.

When confocal images were used to determine the relative intensity of fluorescence in the nucleus (*Fn*) and in the cytoplasm (*Fc*) (Fig. 5A), the *Fn*/*c* ratio increased significantly from about 0.35 for GFP to 1.4 for GFP-NLS (Fig. 5B). Introduction of mutations K18E and K20E in the 3D NLS rendered values similar to those of GFP. Cellular fractions with BHK-21 cells transfected with plasmids expressing the different GFP fusion proteins showed a nuclear/cytoplasmic distribution of GFP staining similar to that determined by inmunofluorescence (Fig. 6). These results confirm that the sequence motif MRKTKLAPT has an intrinsic nuclear localizing ability.

Sequences flanking the MRKTKLAPT motif can increase nuclear targeting of the heterologous protein

As mentioned, the MRKTKLAPT motif in FMDV 3D fits the consensus sequence identified at the 3Dpol N-terminus of other picornaviruses, such as EMCV and rhinovirus, which is similar to the consensus for NLS of yeast ribosomal proteins (YRP-NLS) (Aminev et al., 2003b; Stuger et al., 2000). In some of these proteins, sequences flanking the NLS motif can enhance the nuclear importation capacity of NLS, improving NLS binding to their receptors, even when they do not contain basic residues or show homology with classical NLS (Garcia-Bustos et al., 1991; Lange et al., 2007). To assess whether sequences flanking the MRKTKLAPT motif increased its capacity to promote nuclear localization, plasmid GFPNLS2 – in which GFP was fused with the 3D sequence spanning the MRKTKLAPT motif plus the 9 flanking amino acids at both of its C-ter and N-ter sides (RDVEERVHV**MRKTKLAPT**VAHGVFNPE) – was constructed (see Fig. 4A). GFP-NLS2 was mainly detected in the nucleus and showed an Fn/c ratio of 2.9, higher than that of GFP-NLS (Figs. 4 and 5B). In addition, GFP-NLS2 was mostly found at the nuclear fraction of transfected cells (Fig. 6). Thus, introduction of 9 amino acids at each end of the MRKTKLAPT motif enhances its effect as a NLS. It has been reported that proteins can harbor multiple partially functional NLS signals, being their effect additive. This means that a given protein may have not a single strong NLS (such as the classical SV40 signal), but can harbor more than one weaker signal, promoting in this way the nuclear import (Garcia-Bustos et al.,, 1991); this possibility remains to be analyzed for FMDV 3D.

Mutations K18E and K20E are detrimental for virus infectivity

To assess the effect of replacements K18E and K20E in 3D in the context of viral infection, those mutations were introduced in the full length infectious clone pMT28 (Toja et al., 1999). The infectivity of mutant RNAs transcribed from the resulting plasmids pMTK18E (RNA K18E) and pMTK20E (RNA K20E) was compared with that of the corresponding parental C-S8c1 RNA derived from plasmid pMT28 (RNAwt). In transfected cells incubated in liquid medium, neither cythopathic effect nor infectious virus were detected up to 72 h post transfection with 1 μg of transcripts from pMT28KE or pMTK20E (see Table 1), while C-S8c1 RNA produced

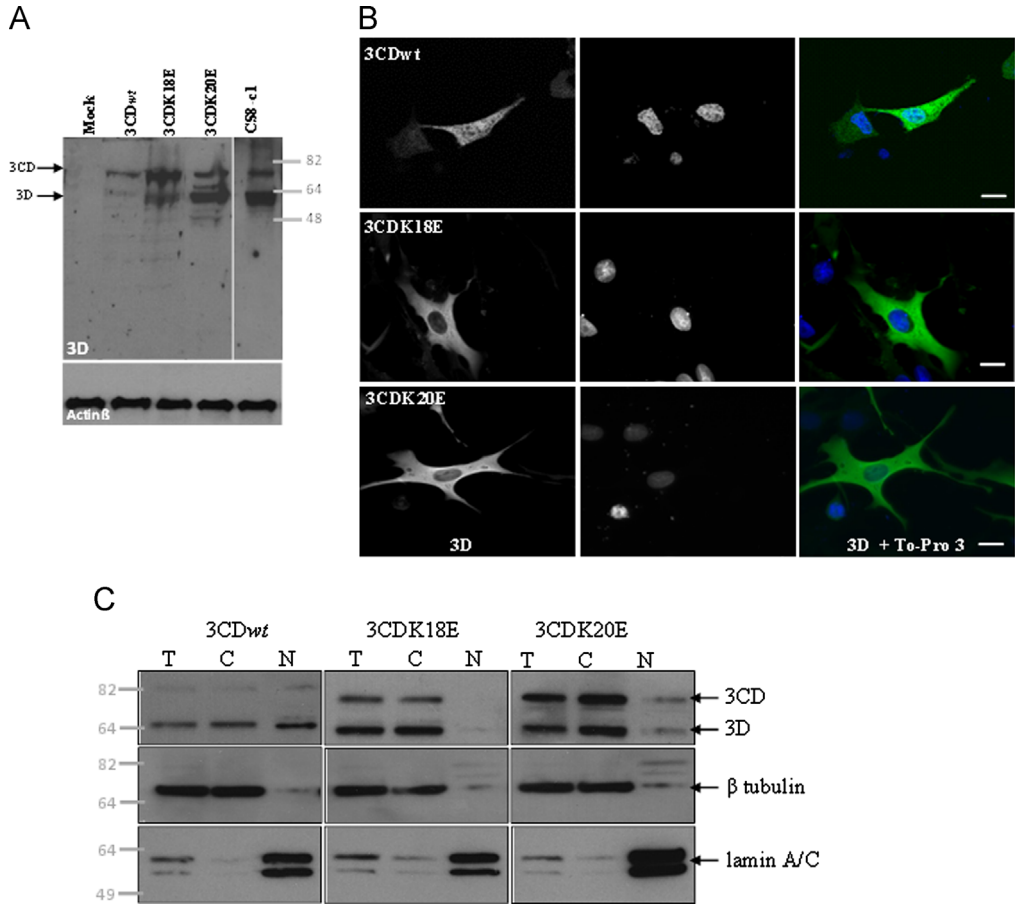

Fig. 3. Cellular localization of 3CD precursor harboring mutations K18E and K20E. BHK-21 cells were electroporated with pRSV-3CD, pRSV-3CDK18E or pRSV-3CDK20E and collected at 20 h post transfection. (A) Expression of the recombinant proteins was detected by western blotting with E56 antibody that recognizes 3D protein. (B) Representative confocal images of 3D distribution. Expression of 3D was detected with serum E56 and Alexa Fluor 488 antirabbit IgGs as secondary antibody; nuclei were stained with To-Pro3. Scale bar: 20 μm. (C) Western blot analysis of cellular fractions of BHK-21 cells transfected with 3D plasmids. At 20 h post transfection, total cell extracts (*T*), cytoplasmic and cell membrane fraction (*C*) and nuclear fraction (*N*) were obtained and blotted (as described in Materials and methods). The migration of the markers and their molecular weight are indicated. Arrows point to the bands corresponding to 3D, 3CDpol, βII-tubulin and lamin *A*/*C*.

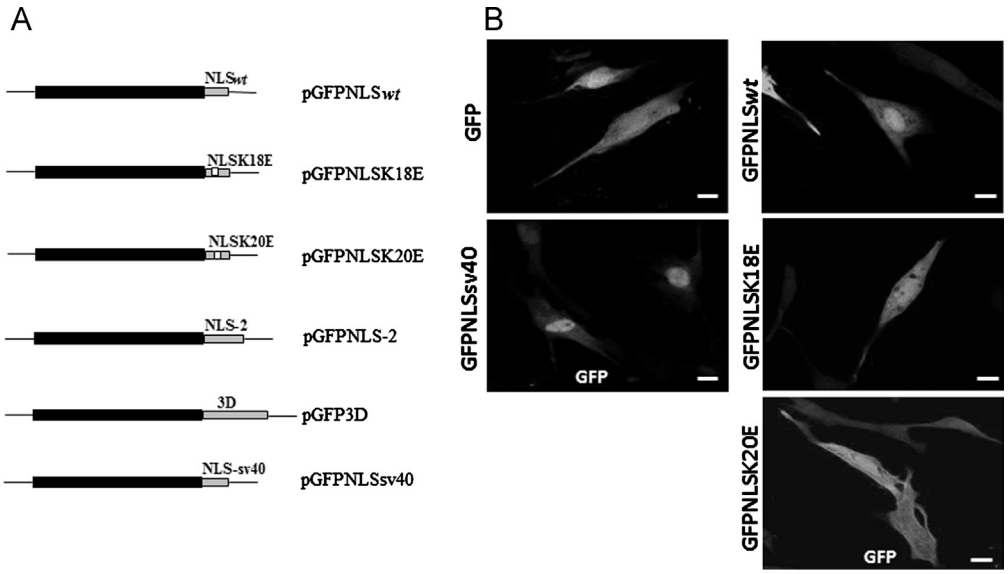

Fig. 4. Expression and localization of GFP-fusion proteins. (A) Scheme of the GFP-fusion proteins used in this study, in which GFP in depicted in black bars. FMDV NLSwt (MRKTKLAPT), NLSK18E, NLSK20E, the complete FMDV 3D sequence, GFPNLS2 (RDVEERVHVMRKTKLAPTVAHGVFNPE) and NLSsv40 (Conti et al., 1998) are indicated by grey bars. (B) Distribution of GFP-NLS proteins by confocal microscopy. Representative images of cells transfected with the plasmids expressing the proteins indicated fixed and processed at 24 h post transfection. Autofluorescence of GFP is shown. Scale bar: 20 μm. (For interpretation of the references to color in this figure legend, the reader is referred to the web version of this article.)

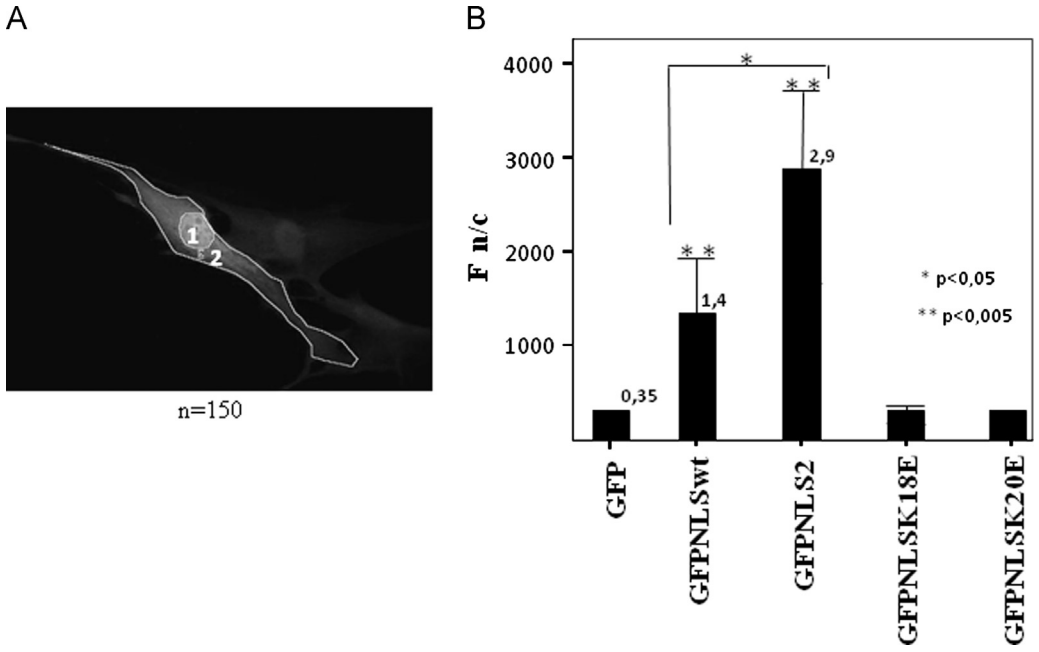

Fig. 5. Nuclear localization of GFP-fusion proteins. A scheme of the fusion proteins used is shown in Fig. 4A. (A) Images such as those shown in Fig. 4B were analysed using the Image J1.62 software to determine the Nuclear/Cytoplasmic fluorescence intensity ratios (*Fn*/*c* ratio). (B) Histogram showing the Fn/c ratio calculated for each group of cells as follows: $Fn/c=(Fn-Fb)/(Fc-Fb)$ where *Fn* is the nuclear fluorescence, *Fc* is the cytoplasmic fluorescence, and *Fb* is the background fluorescence (autofluorescence). Results are expressed as the mean ± standard deviation. Differences are considered statistically significant when $p<0.05$ ($^{*}p<0.05$; $^{**}p<0.005$).

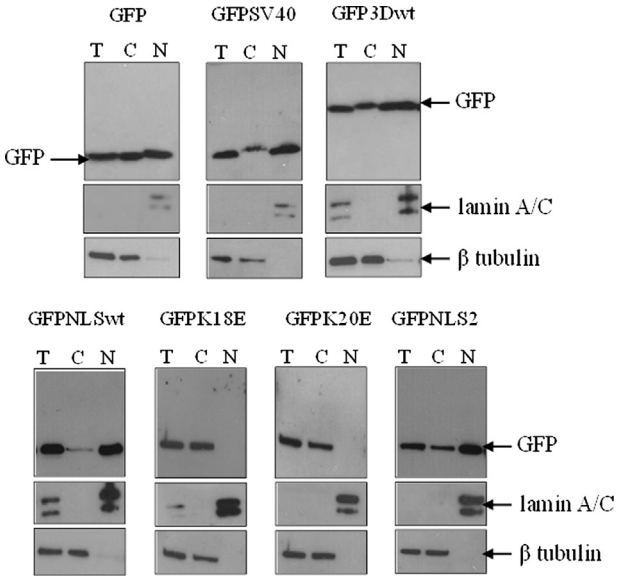

Fig. 6. Western blot analysis of fractions of cells transfected with GFP-fusion proteins. A scheme of the fusion proteins used is shown in Fig. 4A. BHK-21 cells were transfected with different plasmids and collected at 20 h post infection. Total cell extracts (*T*), cytoplasmic and cell membrane fraction (*C*) and nuclear fraction (*N*) were obtained and blotted (as described in Materials and Methods). The migration of the markers and their molecular weight are indicated. Arrows point to the bands corresponding to GFP, βII-tubulin and lamin *A*/*C*.

Table 1
Recovery of infectious virus from RNAs 3DK18E and 3DK20E.

RNA	Transfection			First passage			Second passage		
	24[a]	48	72	24[b]	48	72	24[b]	48	72
None	–[c]	–	–	–	–	–	–	–	–
wt	++++	†[d]	†	++++	†	†	++++	†	†
3DK18E	–	–	–	+	++++	–	–	†	†
3DK20E	–	–	–	–	–	–	–	+	++++

[a] *h* post transfection.
[b] *h* post infection.
[c] CPE produced in BHK-21 cell monolayers at different times post transfection and upon each of two passages of the transfected medium in these cells. Without CPE (–); CPE in about 25% (+), 50% (++), 75% (+++) or 100% (++++) of BHK-21 monolayer. This is a representative example of three independent experiments.
[d] Total CPE at 24 h post transfection.

complete cythopathic affect 24 h post transfection, yielding a viral titer of 5×10^3 PFU/ml. A first passage of the medium of cells transfected with K18E RNA resulted in the emergence of CPE 48 h post infection, which was complete 72 h post infection. For K20E RNA, detection of CPE was only observed in the second passage given to the transfection medium (see Table 1). Emergence of infectious virus was concomitant with the imposition in the viral populations of direct reversions for each of the mutant RNAs analyzed – nucleotide substitutions A6661G and A6667G leading to replacements E18K and E20K, respectively, – that restored the 3D wt sequence, as determined by sequencing of the viral RNA from the infected cell medium. A similar pattern of virus recovery was observed in two additional independent transfections performed with RNAs K18E and K20E. These results indicate that replacements K18E and K20E drastically reduce viral multiplication, leading to selection of viruses with direct reversions that restore the parental K and suggesting that the presence of a positively charged residue at positions 18 and 20 is critical for virus growth. Replacements K18E and K20E are located on the N-terminal domain of the three dimensional structure determined for the 3D protein of C-S8c1 FMDV (Ferrer-Orta et al., 2006). This domain does not directly interact with the active enzymatic site of the protein. Nevertheless, it cannot be excluded that replacements K18E and K20E could affect the replication activity of 3D, as shown for analogous mutations in EMCV 3D protein (Aminev et al., 2003b).

In summary, in this paper, we have confirmed the presence of a NLS in the FMDV 3D protein sequence, which could be responsible

for the nuclear location of 3CD and 3D observed in FMDV transfected and infected cells (Garcia-Briones et al., 2006). While the biological relevance of the presence of 3D in the cell nucleus remains unknown, it has been proposed that nuclear importation of its precursor, 3CD, would allow 3C to contribute to the alterations associated to the nuclear reprogramming occurred upon picornavirus infection (Weidman et al., 2003).

Materials and methods

Cells

The origin and culture procedures for BHK-21 cells have been previously described (Rosas et al., 2008).

Construction of infectious cDNA clones carrying replacements K18E and K20E in 3D, RNA synthesis and transfection

To assess their effect on FMDV infectivity, K18E and K20E mutations were introduced in plasmid pMT28 encoding the type C FMDV isolate C-S8c1 full length sequence (García-Arriaza et al., 2004) by site-directed mutagenesis (Martin-Acebes et al., 2011), To this end, the following pairs of primers were used: 5′-CATG-TAATGCGCGAAACCAAGCTTGCACC-3′ and 5′-GGT GCAAGCTTGG-TTTCGCGCATTACATG-3′ that introduced nucleotide substitution A6661G (replacement K18E), and 5′-TAATGCGCAAAACCGAGCTTG CACCCACC-3′ and 5′-GGTGGGTGCAAG CTCGGTTTTGCGCATTA-3′ that introduced nucleotide substitution A6667G (replacement K20E). The following primers were used for the amplification of the site-directed mutagenesis: 5′- ACGCCGGTCCGATGGAGAGACA-GAAG -3′ and 5′-CCGTTCTCGAAATCGA TAAGTGCACCGC-3′. For RNA synthesis, the resulting plasmids (pMTK18E and pMTK20E) were linearized with NdeI (New England Biolabs) and in vitro transcribed using SP6 RNA polymerase (Promega). After transcription, the reaction mixture was treated with RQ1 DNase (1 U/μg RNA; Promega) and the RNA was extracted with phenol-chloroform and precipitated with ethanol. The RNA integrity and concentration were determined by electrophoresis on agarose gels. In vitro-transcribed RNAs were transfected into BHK-21 cells using the Lipofectin reagent (Invitrogen), as described (Martin-Acebes et al., 2010). Cells were maintained at 37 °C in Dulbecco's modified Eagle's medium (DMEM) supplemented fetal bovine serum (FBS).

Construction of transient expression plasmids

Plasmids for transient expression were derived from plasmid pRSV/L (de Wet et al., 1987) in which the luciferase gene was replaced by the sequences that encoded FMDV C-S8c1 3D and 3CD proteins (García-Arriaza et al., 2004), or the corresponding mutant sequences (3DK18E, 3DK20E, 3CDK18E and 3CDK20E). 3D and 3CD sequences were amplified by PCR from infectious clone pMT28 (Garcia-Arrianza et al., 2004) or plasmids pMTK18E and pMTK20E, using the primers shown in Supplementary material (Table S1), which included restriction sites for cloning into plasmid pRSV/L, HindIII in 5′ and KpnI or SmaI in 3′ sense. Ligation, transformation of E. coli DH5α, colony screening, nucleotide sequencing, were carried out as described (Garcia-Briones et al., 2006). Plamids harbouring fusions with GFP protein (GFPNLS, GFPNLSK18, GFPNLSK20E and GFPNLSsv40) were constructed from plasmid pAcGFP1_c2 (Promega). The sequences of interest were cloned in the extreme carboxi-terminal of GFP protein sequence, with the primers indicated in Table S1. As control, a plasmid expressing GFP protein fused to the SV40 TAg NLS sequence was generated using primers 5′-AATTCCCAAAAAAGAAGAGAAAGGTCC-3′ and 5′- CCCGGGGACCTTTCTC TTCT TTTTTGGG-3′.

Antibodies and reagents

Rabbit polyclonal sera to 3D FMDV protein (E56), was kindly provided by E. Beck (Strebel et al., 1986). The antibodies against GFP and lamin A/C were obtained from Roche and Santa Cruz Biotechnology, respectively. The rabbit polyclonal anti-βII tubulin serum is described in Armas-Portela et al. (1999). Horseradish-peroxidase (HRP)-coupled anti-mouse or anti-rabbit antibodies were from Amersham. Goat antibodies anti-mouse and anti-rabbit IgGs coupled to Alexa 594 or 488 were from Molecular Probes. To-Pro-3 (Molecular Probes) was used for nuclear staining.

Western blot analysis

BHK-21 cell monolayers transfected with the different plasmids were collected 24 h post-transfection in lysis buffer (10 mM EGTA, 2.5 mM MgCl2, 1% NP-40 and 20 mM HEPES, pH 7.4) supplemented with 1 mM PMSF and protease inhibitor cocktail (Roche). Proteins were resolved on a 12% SDS-PAGE and transferred onto a nitrocellulose membrane. After membrane blocking, proteins were detected by incubation with primary antibodies and HRP-coupled anti-mouse or anti-rabbit antibodies using a chemiluminescence kit (Perkin-Elmer) as previously described (Rosas et al., 2008).

Cellular fractionation

BHK-21 cellular fractionation was performed as described before (Garcia-Briones et al., 2006). Briefly, cells transfected were washed with PBS, collected by centrifugation at $110 \times g$ for 5 min and resuspended in 0.25 M sucrose in buffer A (50 mM Tris, 5 mM EDTA, 1 mM $MgCl_2$, 0.5% Triton X-100), supplemented with 1 mM PMSF and protease inhibitor cocktail (Roche). Suspensions were homogenized and nuclei were separated from cytoplasmic and membrane components (cytoplasmic fraction) by centrifugation at $440 \times g$ for 20 min. Protein concentration was determined by Bradford, and equal amounts from each fraction, in Laemmli buffer, were analysed by SDS-polyacrylamide gel electrophoresis, as described above.

Immunofluorescence assays

Immunofluorescence assays were performed as described (Martin-Acebes et al., 2008; Martin-Acebes et al., 2007). Briefly, cells transfected and cultured on coverslips were fixed at 24 h post transfection with 4% paraformaldehyde for 15 min, blocked and permeabilized by incubating in PBTG buffer (0.1% Triton X-100, 1% bovine serum albumin, 1 M glycine in PBS) for 15 min at room temperature. Samples were incubated with primary antibodies for 1 h, washed in PBS and incubated with secondary antibodies for 30 min. Nuclear staining with To-Pro-3 (Invitrogen) was performed as recommended by the manufacturer. Samples were then mounted in Fluoromount-G (Southern Biotech).

Determination of N/C (nuclear/cytoplasm) ratios by image analysis

Cells cultured on coverslips were transfected with mutants and stained for immunofluorescence as detailed above. Confocal images were acquired with a Zeiss LSM 510 confocal microscope using the following laser lines: 488 nm (30 mWArgon, 8–10%), 543 nm (1.2 mW HeNe, 30%) and 633 nm (5 mW HeNe, 50%). Cells exhibiting an unusual size, morphology or expression levels were discarded. Images were taken with 63x lens and 488 nm laser line. A single optical slice was chosen and the images obtained were analyzed using the Image J1.62 software to determine the nucleus/cytoplasm ratio, Fn/c ratio: $Fn/c=(Fn-Fb)/(Fc-Fb)$, where Fn is the

nuclear fluorescence, *Fc* is the cytoplasmic fluorescence, and *Fb* is the background fluorescence. In this experiments 150 cells/field were counted.

Viral RNA extraction and sequencing

Viral RNA was extracted from supernatants of cell cultures using TRI Reagent (Sigma), as described by the manufacturer. cDNA was synthesized by reverse transcription of viral RNA using M-MuLV Reverse Transcriptase (Roche) and primers 5′-ACGCCGGTCCGATGGAGAGACAGAAG-3′ and 5′-TATATAGGTACGTG-CGTCGCCGCAC -3′. cDNA spanning nucleotides 5834 (corresponding to residue 3 of 3B2) to 8019 (corresponding to residue 470 of 3D) was amplified by PCR using the same primers and BioTaq DNA Polymerase (Bioline) supplemented with a 10% of Expand High Fidelity Polymerase (Biotools) for proofreading activity. PCR products were purified with Wizard SV Gel and PCR Clean-Up System (Promega) and sequenced using the primers indicated above and primer 3D-1 (Supplementary material, Table S1). DNA sequences were confirmed by at least two independent sequencing reactions. Nucleotide positions correspond to those previously described for FMDV C-S8c1 isolate (N° Genbank AJ133357).

Statistics

To evaluate the statistical significance of the data, one-way analysis of the variance was performed with statistical package SPSS 13.0 (SPSS, Inc) was used. To evaluate the difference in multiple comparisons, pairwise *t*-Student values were calculated by applying Bonferroni's correction. Means ± the standard deviations are represented. The differences were considered statistically significant when $p < 0.05$ ($^{*}p < 0.05$; $^{**}p < 0.005$).

Acknowledgments

We wish to thank Miguel A. Martin-Acebes for his specific advices and ideas, and F. Caridi for her experimental help and discussions. Esteban Domingo for his critical review of the manuscript and valuable comments, and the Microscopy Facility of Centro de Biología Molecular Severo Ochoa (CBMSO). This work was supported by Spanish grants BIO2008-0447-C03-01 and BIO2011-24351, and by an institutional grant from Fundación Ramón Areces.

Appendix A. Supporting information

Supplementary data associated with this article can be found in the online version at http://dx.doi.org/10.1016/j.virol.2013.06.011.

References

Aminev, A.G., Amineva, S.P., Palmenberg, A.C., 2003a. Encephalomyocarditis viral protein 2A localizes to nucleoli and inhibits cap-dependent mRNA translation. Virus Res. 95 (1-2), 45–57.

Aminev, A.G., Amineva, S.P., Palmenberg, A.C., 2003b. Encephalomyocarditis virus (EMCV) proteins 2A and 3BCD localize to nuclei and inhibit cellular mRNA transcription but not rRNA transcription. Virus Res. 95 (1-2), 59–73.

Amineva, S.P., Aminev, A.G., Palmenberg, A.C., Gern, J.E., 2004. Rhinovirus 3C protease precursors 3CD and 3CD' localize to the nuclei of infected cells. J. Gen. Virol. 85 (Pt 10), 2969–2979.

Armas-Portela, R., Parrales, M.A., Albar, J.P., Martínez, A.C., Ávila, J., 1999. Distribution and characteristics of betaII tubulin-enriched microtubules in interphase cells. Exp. Cell Res. 248 (2), 372–380.

Belov, G.A., Evstafieva, A.G., Rubtsov, Y.P., Mikitas, O.V., Vartapetian, A.B., Agol, V.I., 2000. Early alteration of nucleocytoplasmic traffic induced by some RNA viruses. Virology 275 (2), 244–248.

Carrillo, C., Tulman, E.R., Delhon, G., Lu, Z., Carreno, A., Vagnozzi, A., Kutish, G.F., Rock, D.L., 2005. Comparative genomics of foot-and-mouth disease virus. J. Virol. 79 (10), 6487–6504.

Conti, E., Uy, M., Leighton, L., Blobel, G., Kuriyan, J., 1998. Crystallographic analysis of the recognition of a nuclear localization signal by the nuclear import factor karyopherin alpha. Cell 94 (2), 193–204.

de Los Santos, T., de Avila Botton, S., Weiblen, R., Grubman, M.J., 2006. The leader proteinase of foot-and-mouth disease virus inhibits the induction of beta interferon mRNA and blocks the host innate immune response. J. Virol. 80 (4), 1906–1914.

de Los Santos, T., Diaz-San Segundo, F., Grubman, M.J., 2007. Degradation of nuclear factor kappa B during foot-and-mouth disease virus infection. J. Virol. 81 (23), 12803–12815.

de los Santos, T., Segundo, F.D., Zhu, J., Koster, M., Dias, C.C., Grubman, M.J., 2009. A conserved domain in the leader proteinase of foot-and-mouth disease virus is required for proper subcellular localization and function. J. Virol. 83 (4), 1800–1810.

de Wet, J.R., Wood, K.V., DeLuca, M., Helinski, D.R., Subramani, S., 1987. Firefly luciferase gene: structure and expression in mammalian cells. Mol. Cell. Biol. 7 (2), 725–737.

Falk, M.M., Grigera, P.R., Bergmann, I.E., Zibert, A., Multhaup, G., Beck, E., 1990. Foot-and-mouth disease virus protease 3C induces specific proteolytic cleavage of host cell histone H3. J. Virol. 64 (2), 748–756.

Ferrer-Orta, C., Arias, A., Agudo, R., Pérez-Luque, R., Escarmís, C., Domingo, E., Verdaguer, N., 2006. The structure of a protein primer-polymerase complex in the initiation of genome replication. EMBO J 25 (4), 880–888.

García-Arriaza, J., Manrubia, S.C., Toja, M., Domingo, E., Escarmís, C., 2004. Evolutionary transition toward defective RNAs that are infectious by complementation. J. Virol. 78 (21), 11678–11685.

García-Arriaza, J., Manrubia, S.C., Toja, M., Domingo, E., Escarmís, C., 2004. Evolutionary transition toward defective RNAs that are infectious by complementation. J. Virol 78, 11678–11685.

Garcia-Briones, M., Rosas, M.F., Gonzalez-Magaldi, M., Martin-Acebes, M.A., Sobrino, F., Armas-Portela, R., 2006. Differential distribution of non-structural proteins of foot-and-mouth disease virus in BHK-21 cells. Virology 349 (2), 409–421.

García-Briones, M., Rosas, M.F., González-Magaldi, M., Martín-Acebes, M.A., Sobrino, F., Armas-Portela, R., 2006. Differential distribution of non-structural proteins of foot-and-mouth disease virus in BHK-21 cells. Virology 349 (2), 409–421.

Garcia-Bustos, J., Heitman, J., Hall, M.N., 1991. Nuclear protein localization. Biochim. Biophys. Acta 1071 (1), 83–101.

Garrido-Garcia, A., Andres-Pans, B., Duran-Trio, L., Diez-Guerra, F.J., 2009. Activity-dependent translocation of neurogranin to neuronal nuclei. Biochem. J. 424 (3), 419–429.

Grigera, P.R., Tisminetzky, S.G., 1984. Histone H3 modification in BHK cells infected with foot-and-mouth disease virus. Virology 136 (1), 10–19.

Groppo, R., Brown, B.A., Palmenberg, A.C., 2011. Mutational analysis of the EMCV 2A protein identifies a nuclear localization signal and an eIF4E binding site. Virology 410 (1), 257–267.

Gustin, K.E., Sarnow, P., 2001. Effects of poliovirus infection on nucleo-cytoplasmic trafficking and nuclear pore complex composition. EMBO J. 20 (1-2), 240–249.

Kalderon, D., Roberts, B.L., Richardson, W.D., Smith, A.E., 1984. A short amino acid sequence able to specify nuclear location. Cell 39 (3 Pt 2), 499–509.

Kitching, R.P., 2005. Global epidemiology and prospects for control of foot-and-mouth disease. Curr. Top. Microbiol. Immunol. 288, 133–148.

Lange, A., Mills, R.E., Lange, C.J., Stewart, M., Devine, S.E., Corbett, A.H., 2007. Classical nuclear localization signals: definition, function, and interaction with importin alpha. J. Biol. Chem. 282 (8), 5101–5105.

Lawrence, P., Rieder, E., 2009. Identification of RNA helicase A as a new host factor in the replication cycle of foot-and-mouth disease virus. J. Virol. 83 (21), 11356–11366.

Lawrence, P., Schafer, E.A., Rieder, E., 2012. The nuclear protein Sam68 is cleaved by the FMDV 3C protease redistributing Sam68 to the cytoplasm during FMDV infection of host cells. Virology 425 (1), 40–52.

Martin-Acebes, M.A., Gonzalez-Magaldi, M., Rosas, M.F., Borrego, B., Brocchi, E., Armas-Portela, R., Sobrino, F., 2008. Subcellular distribution of swine vesicular disease virus proteins and alterations induced in infected cells: a comparative study with foot-and-mouth disease virus and vesicular stomatitis virus. Virology 374 (2), 432–443.

Martin-Acebes, M.A., Gonzalez-Magaldi, M., Sandvig, K., Sobrino, F., Armas-Portela, R., 2007. Productive entry of type C foot-and-mouth disease virus into susceptible cultured cells requires clathrin and is dependent on the presence of plasma membrane cholesterol. Virology 369 (1), 105–118.

Martín-Acebes, M.A., Rincón, V., Armas-Portela, R., Mateu, M.G., Sobrino, F., 2010. A single amino acid substitution in the capsid of foot-and-mouth disease virus can increase acid-lability and confer resistance to acid-dependent uncoating inhibition. J. Virol 84, 2902–2912.

Martín-Acebes, M.A., Vázquez-Calvo, A., Rincón, V., Mateu, M.G., Sobrino, F., 2011. A single amino acid substitution in the capsid of foot-and-mouth disease virus can increase acid-lability and confer resistance to acid-dependent uncoating inhibition. J. Virol 85, 2733–2740.

Martínez-Salas, E., Domingo, E., 1995. Effect of expression of the aphthovirus protease 3C on viral infection and gene expression. Virology 212 (1), 111–120.

Newman, J.F., Cartwright, B., Doel, T.R., Brown, F., 1979. Purification and identification of the RNA-dependent RNA polymerase of foot-and-mouth disease virus. J. Gen. Virol. 45 (2), 497–507.

Nigg, E.A., 1997. Nucleocytoplasmic transport: signals, mechanisms and regulation. Nature 386 (6627), 779–787.

Rosas, M.F., Vieira, Y.A., Postigo, R., Martín-Acebes, M.A., Armas-Portela, R., Martínez-Salas, E., Sobrino, F., 2008. Susceptibility to viral infection is enhanced by stable expression of 3A or 3AB proteins from foot-and-mouth disease virus. Virology 380 (1), 34–45.

Ryan, M.D., Donnelly, M.L.L., Flint, M., Cowton, V.M., Luke, G., Hughes, L.E., Knox, C., De Felipe, P., 2004. In: Sobrino, F., Domingo, E. (Eds.), Foot-and-mouth disease virus proteinases. In: Foot and Mouth Disease: Current Perspectives. Horizon Bioscience, Norfolk.

Sáiz, M., Nuñez, J.I., Jiménez-Clavero, M.A., Baranowski, E., Sobrino, F., 2002. Foot-and-mouth disease virus: biology and prospects for disease control. Microbes Infect. 4 (11), 1183–1192.

Strebel, K., Beck, E., Strohmaier, K., Schaller, H., 1986. Characterization of foot-and-mouth disease virus gene products with antisera against bacterially synthesized fusion proteins. J. Virol. 57 (3), 983–991.

Stuger, R., Timmers, A.C., Raue, H.A., Van't Riet, J., 2000. Nuclear import of ribosomal proteins: evidence for a novel type of nuclear localization signal. In". In: Garret, R.A., Douthwaite, A., Liljas, A.T., Matheson, P.B., Moore, P.B., Noller, H.F. (Eds.), The Ribosome Structure, Function, Antibiotics and Cellular Interactions. ASM Press, Washington, D.C..

Terry, L.J., Shows, E.B., Wente, S.R., 2007. Crossing the nuclear envelope: hierarchical regulation of nucleocytoplasmic transport. Science 318 (5855), 1412–1416.

Toja, M., Escarmis, C., Domingo, E., 1999. Genomic nucleotide sequence of a foot-and-mouth disease virus clone and its persistent derivatives. Implications for the evolution of viral quasispecies during a persistent infection. Virus Res 64, 161–171.

Wang, D., Fang, L., Luo, R., Ye, R., Fang, Y., Xie, L., Chen, H., Xiao, S., 2010. Foot-and-mouth disease virus leader proteinase inhibits dsRNA-induced type I interferon transcription by decreasing interferon regulatory factor 3/7 in protein levels. Biochem. Biophys. Res. Commun. 399 (1), 72–78.

Weidman, M.K., Sharma, R., Raychaudhuri, S., Kundu, P., Tsai, W., Dasgupta, A., 2003. The interaction of cytoplasmic RNA viruses with the nucleus. Virus Res. 95 (1-2), 75–85.